Transmission of Microwave Through Perforated Flat Plates of Finite Thickness

CHAO-CHUN CHEN

Abstract—Transmission characteristics of a thick conducting plate perforated with either circular or rectangular holes are presented. Simple explicit formulas for predicting energy leakage through a reflector surface are derived.

Introduction

During the past two decades, metallic sheets perforated with either rectangular or circular holes as shown in Fig. 1 have been widely used to form reflector surfaces, bandpass filters, Fabry–Perot interferometers, and as elements in multipanel filters. Thin perforated sheets are satisfactory for most applications. However, in many cases thick perforated plates are preferred in order to enhance the strength and hardness of the structure, to improve the bandpass filter characteristics, or to avoid radiation hazards due to leakage from microwave sources. Particularly in the millimeter-wave and the far-infrared regions, the thickness of the metallic mesh filter is not negligible compared to the wavelength.

A thick perforated plate exhibits a steeper cutoff between the stop and the passband frequency, which is significant in the design of metallic mesh filters or fenestrated radomes. The thick sheet also finds practical applications in problems associated with the radiation hazards due to leakage through reflective surfaces on low-noise antennas or microwave-oven doors.

Due to the lack of an effective theoretical analysis, a great number of investigations have been performed experimentally [1]–[7]. Those experiments, however, did not provide much information about the thickness effect and its resonant shift with the angle of incidence. Recently, the method of moments has been applied successfully in solving the integral equation for the unknown aperture fields for the case of a thin perforated sheet [8], [9]. This paper extends the numerical method developed for the thin sheet to the case of a thick plate. Transmission properties of a perforated plate at frequencies well below the resonance region are also investigated. Relatively simple explicit formulas for calculating energy leakage through a reflector surface are derived.

General Formula

Consider a thick conducting plate that has symmetrical discontinuities at $z = \pm l_1$. This perforated plate is illuminated by a plane wave at an arbitrary incident angle θ from $z = \infty$. Based on the superposition theorem, this original problem may be decomposed into symmetric and antisymmetric plane-wave excitations. The cases of the symmetric and the antisymmetric excitations are equivalent to open- and short-circuit problems, respectively, at $z = 0$. They will be treated separately as a boundary-value problem. The sum of the two resulting fields is then the solution of the original problem.

Manuscript received October 5, 1971; revised July 3, 1972.

The author is with Hughes Ground Systems, Hughes Aircraft Company, Fullerton, Calif. 92634.

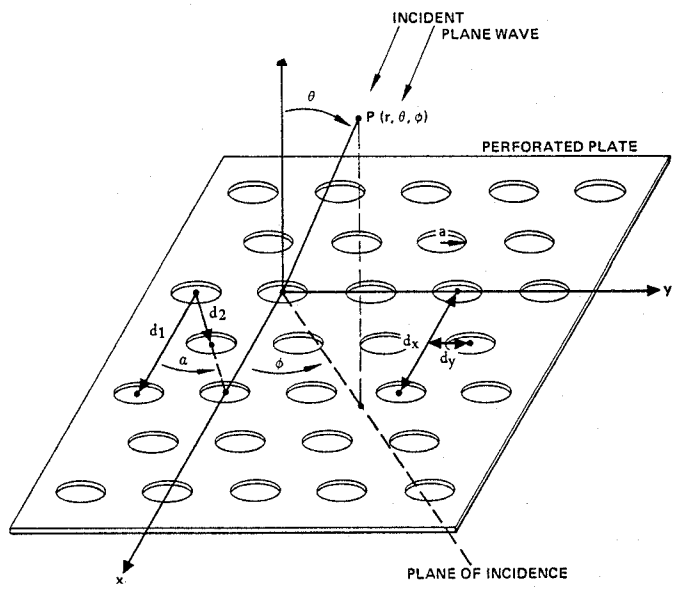

Fig. 1. Geometry of a perforated conducting plate.

To solve the short-circuit or open-circuit boundary-value problem, the fields on both sides of the plate are expanded into a complete set of Floquet modes $\mathbf{\Phi}_{pqr}$, with two spatial harmonic numbers p and q, and a third subscript r, used to denote TE or TM mode. Each Floquet mode has a propagation constant γ_{pq} along the z axis and a characteristic modal wave admittance $\xi_{pqr}{}^f$. The fields inside the holes between two apertures are expressed in terms of the conventional waveguide modes $\mathbf{\Psi}_{mn}$, with a characteristic modal admittance η_{mn} and a propagation constant β_{mn}. The incident wave is of arbitrary polarization with modal voltage coefficients A_{001} and A_{002}. By matching the transverse electric and magnetic fields at the aperture $z = -l_1$, an integral equation for the unknown transverse field at $z = -l_1$ is obtained:

$$2\sum_{r=1}^{2} A_{oor}\xi_{oor}{}^f\mathbf{\Phi}_{oor} = \sum_{r=1}^{2}\sum_{p}^{\infty}\sum_{q}^{\infty}\xi_{pqr}{}^f\mathbf{\Phi}_{pqr}\int\int_{\text{aperture}}\mathbf{\Phi}_{pqr}{}^*\cdot\boldsymbol{E}_t\,da + \sum_{r=1}^{2}\sum_{p}^{\infty}\sum_{q}^{\infty}F_{mnr}Y_{mnr}\mathbf{\Psi}_{mnr}$$
$$p, q = 0, \pm 1, \pm 2, \cdots, \pm\infty$$
$$m, n = 0, 1, 2, \cdots, +\infty \qquad (1)$$

where F_{mnr} and Y_{mnr} are the modal coefficient of the conventional waveguide modes and the input admittance looking into the waveguide from the aperture at $z = -l_1$, respectively. In the cases of open and short circuits at $z = 0$, the input admit-

tance is

$$Y_{mnr} = +j\eta_{mnr}\tan(\beta_{mnr}l_1), \quad \text{for open circuit}$$
$$= -j\eta_{mnr}\cot(\beta_{mnr}l_1), \quad \text{for short circuit.} \quad (2)$$

By substituting (2) into (1), two integral equations, one for the open-circuit and the other for the short-circuit problem, are obtained. The open- and short-circuit aperture fields at $z=-l_1$, $\boldsymbol{E}_o$ and $\boldsymbol{E}_s$ are obtained by solving these two integral equations independently by the method of moments. Thus the transverse aperture fields at $z=\pm l_1$ of the original problem are

$$E_t(z = \mp l_1) = \tfrac{1}{2}[\boldsymbol{E}_o \pm \boldsymbol{E}_s]. \quad (3)$$

The positive sign applies to the aperture field on the incident side of the plate, and the negative sign to the aperture field on the transmitted side. The reflection coefficient at $z=-l_1$ is

$$R_{pqr} = \iint_{\text{aperture}} \boldsymbol{E}_t(z = -l_1)\cdot\boldsymbol{\Phi}_{pqr}^*\,da - \delta_{pq}A_{oor} \quad (4)$$

where $\delta_{pq}=1$ for $p=q=0$, otherwise $\delta_{pq}=0$.

The transmission coefficient at $z=l_1$ is

$$B_{pqr} = \iint_{\text{aperture}} \boldsymbol{E}_t(z = l_1)\cdot\boldsymbol{\Phi}_{pqr}^*\,da. \quad (5)$$

The same procedure applies equally well to the problem of a thick perforated plate laminated between two identical dielectric sheets, which has been treated in [9] and [11].

In the range of passband frequencies, accuracy of the solution depends upon the number of modes remaining in (1) to approximate the respective fields in the aperture and the free-space regions. The criteria in choosing the proper number of modes in these two regions were discussed in detail in [12] and [13] by Mittra and Lee *et al.* Although the general equations (1)–(5) and the method of moments provide an effective means for determining the reflection and the transmission coefficients of a perforated plate, the interest and practice of using (1)–(5) are often hinged on the complexity of programming the multimode computation and its cost in computation. Furthermore, the foregoing formulation does not give much insight into the physical characteristics of the problems. For many applications, such as antenna reflector surfaces or RF isolation screens, simple explicit expressions are available for rapidly obtaining an approximate estimation of the transmission loss through these surfaces.

Mesh Screen for RF Isolation

Most of RF isolation screens or reflector surfaces are perforated with either circular or square openings arranged in either square or equilateral triangular lattice. Since the size of these openings is usually well below cutoff, only the dominate waveguide mode is of significance in the region of these openings. If the number of free-space modes retained in (1) includes the modes whose transverse propagation coefficients are slightly greater than that of the TE_{11} mode for circular holes or TE_{10} mode for square holes beyond cutoff, an approximate solution can be obtained even without resorting to the computer.

For the case of normal incidence, the reflection and the transmission coefficients of a reflector screen can be reduced to the forms

$$R = \frac{1}{1 - j[A + B\tan h(\beta l)]} + \frac{1}{1 - j[A + B\cot h(\beta l)]} - 1 \quad (6)$$

$$T = \frac{1}{1 - j[A + B\tan h(\beta l)]} - \frac{1}{1 - j[A + B\cot h(\beta l)]} \quad (7)$$

where A and B are functions of element spacing and aperture size. Four different patterns of perforated plate that are most commonly used in practice are the following.

1) Circular Openings with Equilateral Triangular Lattice:

$$A = 12\left(\frac{4}{3}\left(\frac{\lambda}{d}\right)^2 - 1\right)^{1/2}\left[\frac{J_1'\left(\frac{4\pi}{\sqrt{3}}\frac{a}{d}\right)}{1 - \left(\frac{4\pi a}{1.841\sqrt{3}d}\right)^2}\right]^2 - \frac{12}{\left(\frac{4}{3}\left(\frac{\lambda}{d}\right)^2 - 1\right)^{1/2}}\left[\frac{J_1\left(\frac{4\pi}{\sqrt{3}}\frac{a}{d}\right)}{\frac{4\pi}{\sqrt{3}}\frac{a}{d}}\right]^2,$$
$$\text{for } a > 0.28d \text{ and } d < 0.57\lambda \quad (8)$$

$$B = 0.33\left(\frac{d}{a}\right)^2\left(\left(\frac{0.293\lambda}{a}\right)^2 - 1\right)^{1/2} \quad (9)$$

$$\beta = \frac{2\pi}{\lambda}\left(\left(\frac{0.293\lambda}{a}\right)^2 - 1\right)^{1/2} \quad (10)$$

where a is the radius of circular apertures and d is the spacing between any two apertures.

2) Circular Openings with Square Lattice:

$$A = 8\left(\left(\frac{\lambda}{d}\right)^2 - 1\right)^{1/2}\left[\frac{J_1'\left(\frac{2\pi}{d}a\right)}{1 - \left(\frac{2\pi a}{1.841d}\right)^2}\right]^2 + 8\left(2\left(\frac{\lambda}{d}\right)^2 - 1\right)^{1/2}\left[\frac{J_1'\left(\frac{2\pi}{d}\sqrt{2}a\right)}{1 - \left(\frac{2\pi\sqrt{2}a}{1.841d}\right)^2}\right]^2 - \frac{8}{\left(\left(\frac{\lambda}{d}\right)^2 - 1\right)^{1/2}}\left[\frac{J_1\left(\frac{2\pi}{d}a\right)}{\frac{2\pi}{d}a}\right]^2 - \frac{8}{\left(2\left(\frac{\lambda}{d}\right)^2 - 1\right)^{1/2}}\left[\frac{J_1\left(\frac{2\pi}{d}\sqrt{2}a\right)}{\left(\frac{2\pi\sqrt{2}a}{d}\right)}\right]^2,$$
$$\text{for } a > 0.28d \text{ and } d < 0.5\lambda \quad (11)$$

$$B = \frac{1.2}{\pi}\left(\frac{d}{a}\right)^2\left(\left(\frac{0.293}{a}\lambda\right)^2 - 1\right)^{1/2}. \tag{12}$$

3) Square Openings with Equilateral Triangular Lattice:

$$A = \left[3\left(\frac{4}{3}\left(\frac{\lambda}{d}\right)^2 - 1\right)^{1/2} - \frac{1}{\left(\frac{4}{3}\left(\frac{\lambda}{d}\right)^2 - 1\right)^{1/2}}\right] \cdot \left[\frac{\cos\left(\frac{\pi a}{d}\right)}{1 - \left(\frac{2a}{d}\right)^2}\right]^2 \left[\frac{\sin\left(\frac{\pi a}{\sqrt{3}d}\right)}{\left(\frac{\pi a}{\sqrt{3}d}\right)}\right]^2 - \frac{2}{\left(\frac{4}{3}\left(\frac{\lambda}{d}\right)^2 - 1\right)^{1/2}}\left[\frac{\sin\left(\frac{2\pi a}{\sqrt{3}d}\right)}{\left(\frac{2\pi a}{\sqrt{3}d}\right)}\right]^2,$$

$$\text{for } a > 0.5d \quad \text{and} \quad d < 0.57\lambda \tag{13}$$

$$B = \frac{\sqrt{3}\,\pi^2}{16}\left(\left(\frac{\lambda}{2a}\right)^2 - 1\right)^{1/2} \tag{14}$$

$$\beta = \frac{2\pi}{\lambda}\left(\left(\frac{\lambda}{2a}\right)^2 - 1\right)^{1/2} \tag{15}$$

where a is the width of the square openings.

4) Square Openings with Square Lattice:

$$A = 2\left(\left(\frac{\lambda}{d}\right)^2 - 1\right)^{1/2}\left[\frac{\cos\left(\frac{\pi a}{d}\right)}{1 - \left(\frac{2a}{d}\right)^2}\right]^2 - \frac{2}{\left(\left(\frac{\lambda}{d}\right)^2 - 1\right)^{1/2}}\left[\frac{\sin\left(\frac{\pi a}{d}\right)}{\left(\frac{\pi a}{d}\right)}\right]^2 + \left[2\left(2\left(\frac{\lambda}{d}\right)^2 - 1\right)^{1/2} - \frac{2}{\left(2\left(\frac{\lambda}{d}\right)^2 - 1\right)^{1/2}}\right] \cdot \left[\frac{\cos\left(\frac{\pi a}{d}\right)}{1 - \left(\frac{2a}{d}\right)^2}\right]^2 \left[\frac{\sin\left(\frac{\pi a}{d}\right)}{\left(\frac{\pi a}{d}\right)}\right]^2,$$

$$\text{for } a > 0.5d \quad \text{and} \quad d < 0.5\lambda \tag{16}$$

$$B = \frac{\pi^2}{8}\left(\frac{d}{a}\right)^2\left(\left(\frac{\lambda}{2a}\right)^2 - 1\right)^{1/2}. \tag{17}$$

Although A and B can also be derived for the case of an arbitrary incidence, the results are no longer simple. Thus we shall resort to the empirical method for the variation of power transmitted from that of the normal incidence. For an obliquely incident plane wave, the energy leakage through a RF screen or reflector surface can be expressed as

$$\begin{aligned}\text{leakage (dB)} &= -20\log\left|T[\cos\theta]^{2(1-p)}\right|, \\ &\qquad \text{for perpendicular polarization} \\ &= -20\log\left|T[\cos\theta]^{-1.5(1-p)}\right|, \\ &\qquad \text{for parallel polarization}\end{aligned} \tag{18}$$

where p is the plate porosity, i.e., the ratio of surface areas between the opening to the unit cell.

Equations (8)–(17) are valid for small openings below the cutoff of all waveguide modes. The accuracy of the solution from (18) is typically better than ± 1.5 dB for incidence angles less than 60° up to a leakage of a 35-dB level. Equations (6) and (7) also serve as a first-order approximation in the range of passband frequencies.

Numerical Results and Discussion

Transmissibility as a function of the angle of incidence, plate thickness, as well as frequency, is presented for several cases of interest. For the plate with rectangular openings, the criteria given by Mittra [12] and Lee [13] was used to choose the proper number of modes in the two respective regions. For the plate with circular openings, the accuracy of the computed results was verified by examining the conservation of energy, convergence of solution, and observing the higher order mode coefficients [12]. Excellent agreement between the computed and experimental results has been obtained. Fig. 2 shows a comparison of the measured and computed results for a plane wave at normal and 45° incidence. The theoretical curves are the results of 10 waveguide-mode computations.

Effects of conducting plate thickness on the behavior of transmission and reflection are the problems of primary interest in this paper. Consider the case of rectangular waveguides flush-mounted between two parallel ground planes, which may possibly be used as a feed through lens in phased arrays or filters in an oversized beam waveguide in the optical- and millimeter-wave regions. Dimensions of the aperture and its array spacings are

$$a = 0.93 \text{ in} \quad b = 0.278 \text{ in}$$
$$d_x = 1.18 \text{ in} \quad d_y = 0.34 \text{ in} \quad \alpha = 30°$$

for plate thickness from zero to 1.3 free-space wavelengths. Reflection coefficients as a function of plate thickness are plotted in Fig. 3 for a plane-wave incident normally. The cutoff frequency, both phase and amplitude, of the reflection coefficient exhibits a periodic characteristic. The first cycle of this periodicity is approximately but not equal to the rectangular guide wavelength. This is to be expected since there are higher order mode interactions between two apertures when the plate is thin. Below the cutoff frequency, the power reflection coefficient increases with thickness as the coefficient of the 4- and 6-GHz cases. In both cases, the incident waves are totally reflected if the plate is sufficiently electrically thick. However, the phase shifts of the electric field on total reflection are less than 180°, i.e., inductive surfaces. At 6 GHz the phase of the reflected wave asymptotically approaches 90° when the plate becomes very thick.

The reflectivity and transmissibility of a perforated plate depends on both the polarization and the angle of incidence.

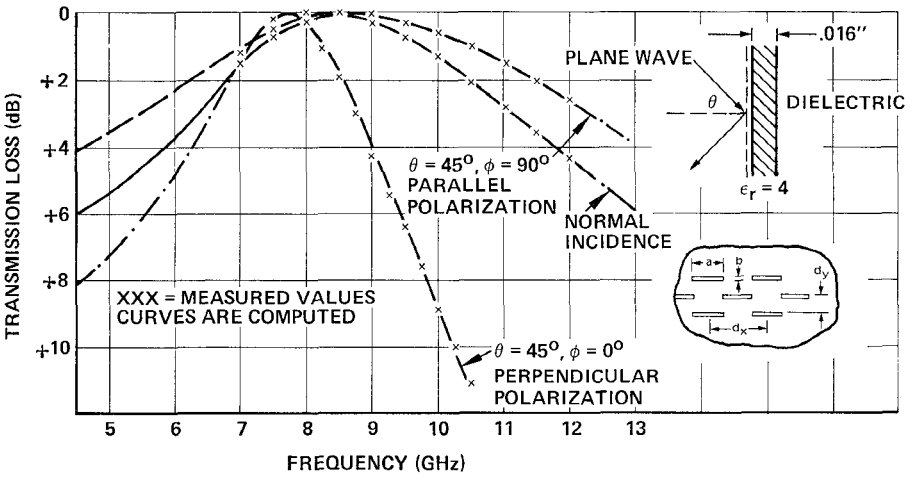

Fig. 2. Comparison of measured and computed transmission losses ($a = 2/3\ d_x$; $b = 1/10\ d_x$; $d_x = 0.9375$ in; $d_y = 1/3\ d_x$.

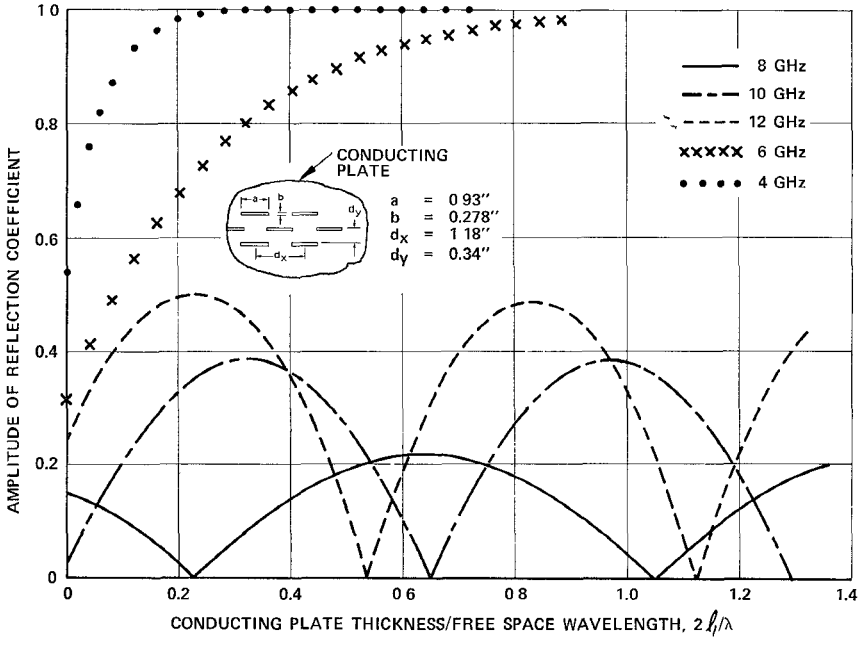

(a)

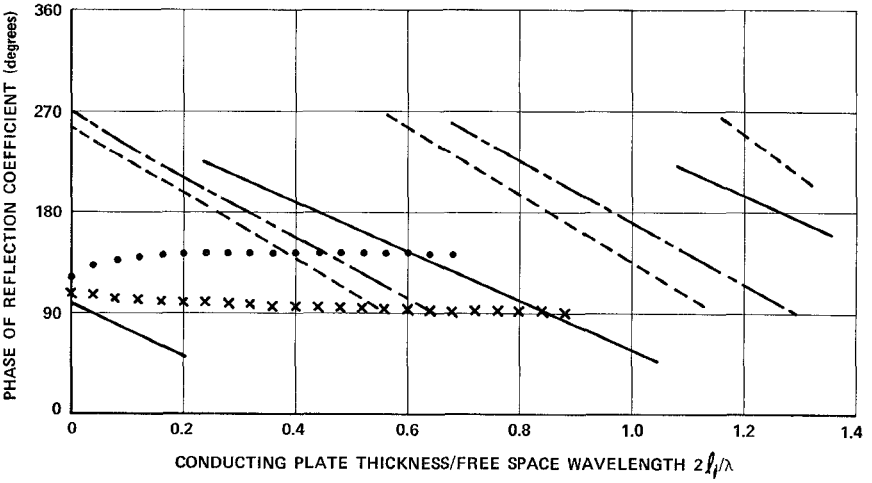

(b)

Fig. 3. (a) Amplitude of reflection coefficient. (b) Phase of reflection coefficient.

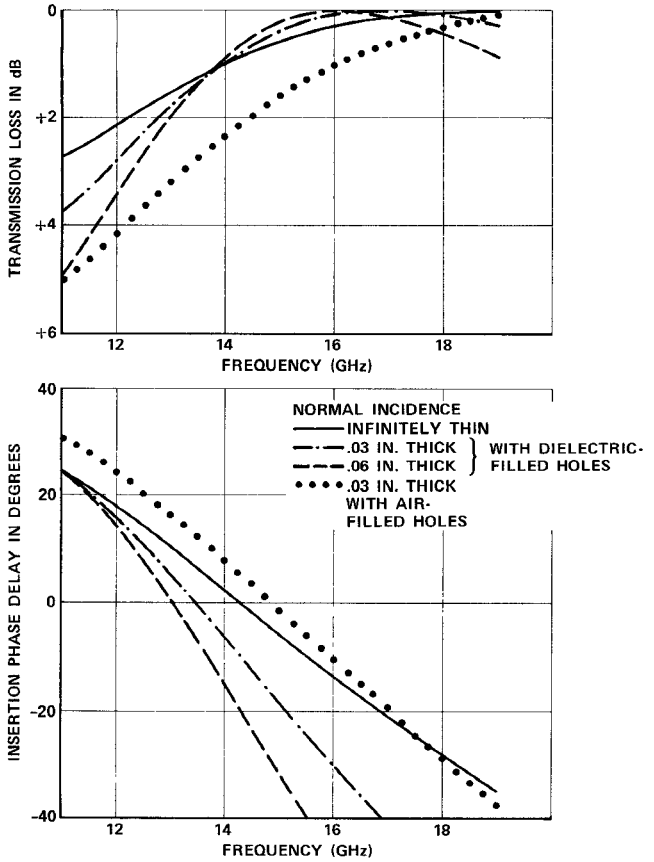

Fig. 4. Transmission loss of a sandwiched flat plate with circular holes versus frequency. $a = 0.159$ in; $d_1 = d_2 = 0.35$ in; $\alpha = 60°$, sandwiched between dielectric sheets 0.028 in thick with $\epsilon_r = 3$ for normal incidence in $\phi = 0°$ plane.

As an example, consider three flat brass plates 0, 0.03, and 0.06 in thick perforated with circular apertures of 0.159-in radius. These apertures are arranged in an equilateral triangular lattice and covered with a dielectric sheet with $\epsilon_r = 3$ and 0.028 in thick on each side. These dimensions were taken after [5], which may be of interest to those involved in bandpass radome design. Fig. 4 shows the insertion loss and the insertion phase delay as functions of frequency at normal incidence. Fig. 5 shows the comparison of insertion loss for perpendicularly and parallel polarized plane waves incident at a $\theta = 60°$ angle. A distinctive difference in resonant shift is observed between the cases with circular holes filled with dielectric and filled with air. For perpendicular polarization, as the angle of incidence increases both resonant frequency and bandwidth decrease from those of the normal incidence. The bandpass behavior also varies with the plane of incidence. However, this variation is minimized in an equilateral triangular lattice arrangement. Computed results on an 0.01-in-thick plate are in agreement with the measured data reported in [5].

The last example considers a perforated plate, which is of interest to those concerned with the microwave leakage through the antenna reflector surfaces or RF screen. Comparison of transmission losses obtained from the 10 lowest order aperture modes by (1), and results from the single-mode calculation from (18) are shown in Fig. 6(a) and (b) for plates with 84-percent and 51-percent porosity, respectively. For the hexagonal lattice considered here, variation of insertion loss versus angle of incidence is insensitive to the plane of incidence. As the angle of incidence increases, the energy leakage

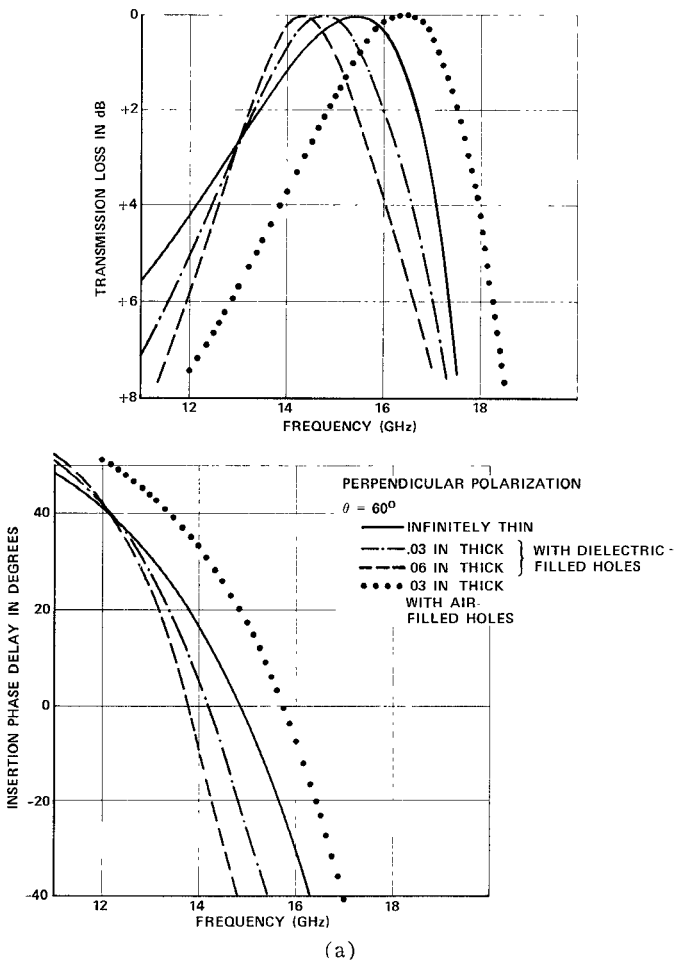

Fig. 5. Transmission loss of a sandwiched flat plate with circular holes versus frequency. $a = 0.159$ in; $d_1 = d_2 = 0.35$ in; $\alpha = 60°$, sandwiched between dielectric sheets 0.028 in thick and with $\epsilon_r = 3$ for $\theta = 60°$ incidence in $\phi = 0°$ plane.

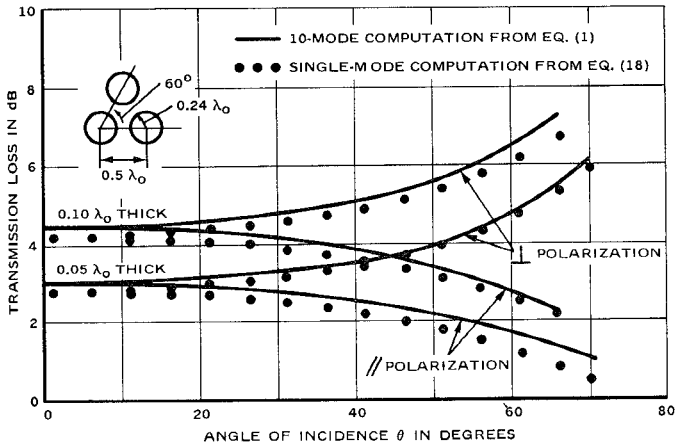

(a)

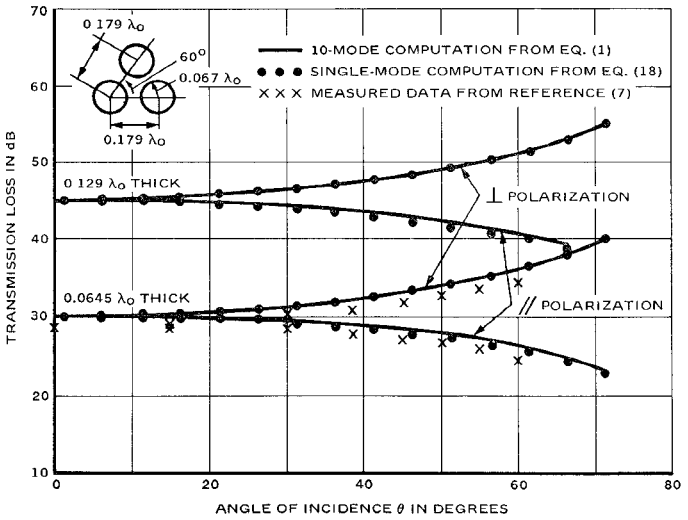

(b)

Fig. 6. (a) Flat perforated plate with 84-percent porosity. (b) Flat perforated plate with 51-percent porosity.

becomes higher than that of the normal incidence for perpendicular polarization, and becomes lower for the parallel polarization. The insertion loss is inversely proportional to the plate thickness. In general, the single-mode aperture field approximation is adequate for calculation of energy leakage through a perforated screen when the size of the apertures are smaller than that of the resonant aperture. Deviations between the computed curves and the measured points are possibly due to the rounded edges of the apertures on tested samples.

Conclusion

In the past, most filter and reflector surfaces have been designed experimentally because there were no accurate theoretical models. It has been demonstrated that this model accurately predicts the performance of a thick plate perforated with either rectangular or circular apertures ranging from electrically small to resonant apertures. Equations (6)–(18) are useful for evaluating energy leakage through reflector surfaces. They also serve as a first-order solution for a perforated plate in the resonance region. Thick plates provide a sharper cutoff between stopband and passband, but the passband narrows as plate thickness increases. Shifts of resonant frequency and changes of bandwidth in the opposite sense for the perpendicular and the parallel polarizations as functions of incident angle limit many useful applications of this perforated plate.

References

[1] P. Vogel and L. Genzel, "Transmission and reflection of metallic mesh in the far infrared," *Infrared Phys.*, vol. 4, pp. 257–262, 1964.
[2] A. Mitsuishi, Y. Otsuka, S. Fujita, and H. Yoshinaga, "Metal mesh filters in the far infrared region," *Japan. J. Appl. Phys.*, vol. 2, pp. 574–577, Sept. 1963.
[3] R. J. Bell and H. V. Romero, "A study of an array of square openings," *Appl. Opt.*, vol. 9, pp. 2341–2349, Oct. 1970.
[4] E. B. McMillan, "Millimeter/microwave radome building block—A dielectric sandwiched metallic circular hole lattice," Resources Develop. Inst., Final Rep. 93101, Oct. 1969.
[5] E. R. Rope, T. E. Fiscus, and G. Tricoles, "Perforated metallic shells for radome applications," General Dynamics, Tech. Rep. R-70-032-F, July 1971.
[6] K. Rogers, J. Montgomery, and D. Purinton, "Slotted metallic RF window investigation," Texas Instruments, Inc., Dallas, Tex., Tech. Rep. AFAL-TR-70-13, June 1970.
[7] K. Woo and T. Y. Otoshi, "RF study of reflector surface materials for rigid and unfurlable antennas," presented at the 1971 G-AP Int. Symp., Los Angeles, Calif., Sept. 1971; data obtained through private correspondence.
[8] C. C. Chen, "Transmission through a conducting screen perforated periodically with apertures," *IEEE Trans. Microwave Theory Tech.*, vol. MTT-18, pp. 627–632, Sept. 1970.
[9] ——, "Diffraction of electromagnetic waves by a conducting screen perforated periodically with circular holes," *IEEE Trans. Microwave Theory Tech.*, vol. MTT-19, pp. 475–481, May 1971.
[10] R. F. Harrington, *Field Computation by Moment Method.* New York: Macmillan, 1964.
[11] N. Amitay and V. Galindo, "Characteristics of dielectric loaded and covered circular waveguide phased arrays," *IEEE Trans. Antennas Propagat.*, vol. AP-17, pp. 722–729, Nov. 1969.
[12] R. Mittra, T. Itoh, and T.-S. Li, "Analytical and numerical studies of the relative convergence phenomenon arising in the solution of an integral equation by the moment method," *IEEE Trans. Microwave Theory Tech.*, vol. MTT-20, pp. 96–104, Feb. 1972.
[13] S. W. Lee, W. R. Jones, and J. J. Campbell, "Convergence of numerical solutions of iris-type discontinuity problems," *IEEE Trans. Microwave Theory Tech.*, vol. MTT-19, pp. 528–536, June 1971.
[14] T. Y. Otoshi, "A study of microwave leakage through perforated flat plates," *IEEE Trans. Microwave Theory Tech.* (Short Papers), vol. MTT-20, pp. 235–236, Mar. 1972.
[15] S.-W. Lee, "Scattering by dielectric-loaded screen," *IEEE Trans. Antennas Propagat.*, vol. AP-19, pp. 656–665, Sept. 1971.